Cable Health Monitoring in Distribution Networks using Power Line Communications

Yinjia Huo, Gautham Prasad, Lutz Lampe, and Victor C. M. Leung
Department of Electrical and Computer Engineering, The University of British Columbia
Email: {yortka, gauthamp, lampe, vleung}@ece.ubc.ca

***Abstract*—Power Line Communication (PLC) harnesses the existing infrastructure of power lines for data transmission. As one application, PLC is being used for monitoring and control in distribution networks. In this paper, we propose an autonomous technique that exploits the communication channel estimated inside legacy PLC modems to determine the health of distribution cables. In particular, we consider paper insulated lead covered (PILC) cables widely used in low- and medium-voltage distribution networks that are most susceptible to thermal degradations. Measurement campaigns have shown that these thermal degradations cause dielectric property changes in PILC cable insulations, which also result in changes in PLC channel conditions. However, through channel characterization of healthy and degraded cables, we demonstrate that the estimated channel frequency responses are not sufficiently distinctive for manual diagnosis. We therefore propose a machine-learning based technique that not only achieves our set target, but is also able to estimate the cable health under varying load conditions. Simulation results show that our proposed technique accurately estimates thermal degradation severities in PILC cables. We thus believe that PLC based cable health monitoring can be used as an autonomous remote diagnostics method that can be integrated into a smart-grid concept and has the promise of being more cost-effective than deploying personnel and/or dedicated equipment.**

I. Introduction

An important constituent of utility assets are the power cables, which are increasingly being deployed underground due to their robustness to weather conditions, reduced impact on the environment, and improved aesthetics in dense neighborhoods [1], [2]. Constant monitoring of cable health is critical, since the smart-grid is expected to essentially provide utilities with complete control and visibility over their assets and services using information and communication technology [3]. Consistent surveillance of power cables enables utilities to prevent cable in-service failures, which can potentially lead to hazardous situations and huge financial losses [4].

As the cable aging progresses, the dielectric properties of the cable insulation continuously deteriorate [5, Ch. 2, Ch. 7], [6]. Consequently, this deterioration manifests itself as changes in the broadband power line communication (BB-PLC) channel [7], [8]. We exploit this principle in our paper to devise a cable health monitoring scheme by inspecting the communication channel estimates computed inside the power line modems (PLMs).

This work was supported by the Natural Sciences and Engineering Research Council of Canada (NSERC).

Using PLC for cable condition monitoring provides several benefits. By reusing the existing grid infrastructure for advanced grid control and communications in the distribution network, PLC has been widely deployed, e.g., in relaying smart metering data to substations with smart meter gateways as data concentration centers [9]–[13]. This minimizes the device installation costs required for cable diagnostics. Furthermore, enabling PLMs with grid sensing abilities can be achieved by using the communication channel state information that is already estimated inside legacy PLMs, and hence imposes no additional hardware modifications. Finally, PLMs allow us to design online diagnostics solutions that can be remotely performed off-site without de-energizing any part of the grid.

In our previous works, we have designed PLM-based diagnostics schemes for extruded cables, where cable aging is mainly caused by electrical degradations, including water-treeing, electrical-treeing, and partial discharge [8], [14], [15]. However, the electrical stress imposed in low-voltage (LV) grid is below the critical value for the inception of electrical degradations [16]. In this paper, we investigate the applicability of using PLMs to design techniques that can diagnose thermal degradations, which is the main aging mechanism in paper insulated lead covered (PILC) cables that are widely deployed in both LV distribution networks [14], [17], as well as medium-voltage (MV) distribution networks [18], [19].

Based on measurements reported in the literature, we first develop a thermal aging model to characterize dielectric properties of a PILC cable susceptible to the thermal aging. Next, we use multi-conductor transmission line (MTL) theory to model PLC channels and generate channel frequency responses (CFRs) of healthy and degraded cables. Through this process, we show that the difference between the cable CFRs under healthy and degraded conditions are insignificant to the naked eye, which renders manual diagnosis hardly feasible for this scenario. To address this issue, as well as to counter situations where CFR changes could be caused by other factors, such as changing load conditions, we use machine-learning (ML) techniques to monitor the cable health by predicting its thermal degradation severity level. ML techniques used in some form for grid diagnostics have been widely applied in the past, e.g., [8], [15], [20], [21]. However, in this paper, we detail the procedure to choose the right features extracted from the estimated CFRs to predict the extent of thermal degradations. Finally, we present a discussion on our proposed solution,

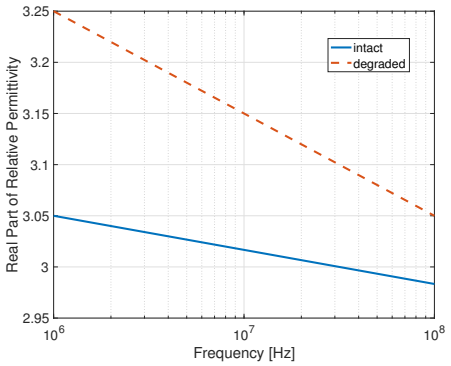

Fig. 1. Extrapolated values of the real part of the relative permittivity of the insulation.

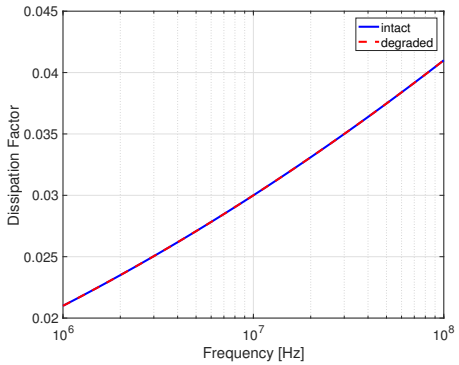

Fig. 2. Extrapolated dissipation factor values of the insulation.

including its applicability using narrowband PLC (NB-PLC) modems, which are widely used for communication between smart meters and secondary transformers in LV networks [22].

Nomenclature: We use $\Re\{x\}$ and $\Im\{x\}$ to denote the real and imaginary parts of a complex number x, respectively.

II. Modeling Thermal Aging

Thermal degradations are internal effects on the insulation caused by long term elevated operating temperature [23]. During the process of thermal aging, the chemical properties of the insulation material continuously change, and the mechanical and electrical properties of the insulation material continuously deteriorate [17]. While most of the existing work on thermal aged PILC cable dielectric property characterization provide measurement results in the low frequency range (up to 1 kHz) [17]–[19], the measurements in [24] cover a broader frequency range from 10^{-2} Hz to 1 MHz. Furthermore, since the trends of the relative permittivity and the dissipation factor (DF) stabilize with increasing frequency, we extrapolate these values to obtain a thermal aging model covering our considered BB-PLC operating band of $2-30$ MHz [25], [26]. Specifically, for the healthy and degraded samples in [24, Fig. 2 and Fig. 10], we use linear extrapolation for the real part of the relative permittivity and quadratic extrapolation for the DF to obtain the results shown in Fig. 1 and Fig. 2, respectively. Note that the measurement results vary with operating temperature. Since the maximum operating temperature of a PILC cable is typically $80°$C [23], we use the measurement results for an operating temperature between $50-70°$C.

The results of Fig. 1 and Fig. 2 are based on the measurements provided in [24], where a degradation was introduced in the cable through manually accelerated thermal aging of nine days. Following this, we denote the real parts of measured relative permittivity and DF subject to a degradation severity level γ as $\epsilon'_{\mathsf{PILC}}(\gamma)$ and $\tan\delta(\gamma)$, respectively, where $\gamma = 0$ represents an intact condition and $\gamma = 1$ represents the nominal degradation severity level after manually accelerated thermal aging of nine days. However, as Fig. 2 shows, thermal degradation does not cause any noticeable changes in DF. Therefore, we let $\tan\delta(\gamma) = \tan\delta$ throughout the rest of the paper. We then compute the imaginary part of the relative permittivity associated with a degradation severity of γ as

$$\epsilon''_{\mathsf{PILC}}(\gamma) = \epsilon'_{\mathsf{PILC}}(\gamma) \cdot \tan\delta, \tag{1}$$

and the final complex relative permittivity of the PILC cable insulation as

$$\epsilon_{\mathsf{PILC}}(\gamma) = \epsilon'_{\mathsf{PILC}}(\gamma) - j\epsilon''_{\mathsf{PILC}}(\gamma), \tag{2}$$

where $j = \sqrt{-1}$.

TABLE I
Properties of the BS6480 Three-core PILC Cable [29]

Conductance separation (d_{cond})	12.28 mm
Conductance radius (r_{cond})	3.34 mm
Copper conductance (σ_{cond})	5.96×10^7 S/m
Normal Operating Voltage	6.35 kV
Maximum Rated Voltage	11 kV
Maximum Operating Temperature	$80°$C

III. PLC Channel Modeling

Having obtained ϵ_{PILC} under different degradation severities, we use a bottom-up approach to generate the CFRs. The cable can be viewed as a uniform line with electrically small cross-sectional dimensions, in which case, the PLC signal propagation can be assumed to follow the quasi-transverse-electromagnetic (quasi-TEM) mode, and the PLC channel can be modeled using the MTL theory [27].

The solution of the MTL equations require the per-unit-length (PUL) parameters that capture all the cross sectional information about the cable [28, Ch. 1]. Therefore, we first determine the PUL parameters, namely, line resistance ($\mathbf{R}$), line inductance ($\mathbf{L}$), shunt capacitance ($\mathbf{C}$), and shunt conductance ($\mathbf{G}$) matrices for the given cable.

We consider a three-conductor PILC mains power distribution cable BS6480 [29], whose normal operating voltage and maximum rated voltage allows us to use it in both LV and MV networks. The cable parameters are listed in Table I for reference. Of the three conductors, we assign an arbitrary one as the reference and denote it as the 0th conductor, and the remaining two as the 1st and 2nd conductors. For the

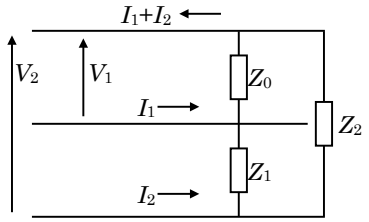

Fig. 3. The load condition at the receiver-end of the line.

ith conductor, the PUL resistance, R_i $(0 \leq i \leq 2)$, can be computed by considering the skin effect as [28, Eq. 4.103b]

$$R_i = \frac{1}{2r_i\pi\sigma_{\mathsf{cond}}\Lambda}, \tag{3}$$

where $r_i = r_{\mathsf{cond}}$ (see Table I) is the radius of the i-th conductor and Λ is the skin depth defined as

$$\Lambda = \frac{1}{\sqrt{\mu\pi f\sigma_{\mathsf{cond}}}}, \tag{4}$$

where μ is the permeability of the insulation material, which, for our cable is that of free space, i.e., $\mu = \mu_0 = 4\pi \times 10^{-7}$ H $\cdot$ m^{-1}, since paper insulation is non-ferromagnetic in nature, and σ_{cond} is the conductivity of the copper conductor. Note that (3) is valid when $\Lambda \ll r_i$, which holds true for our considered cable and the operating frequency range. The PUL resistance matrix can then represented as [28, Eq. 3.12]

$$\mathbf{R} = \begin{bmatrix} R_0 + R_1 & R_0 \\ R_0 & R_0 + R_2 \end{bmatrix}. \tag{5}$$

Since the paper insulation is non-ferromagnetic, the surrounding medium can also be deemed as free space for the purposes of computing the inductance matrix. In such a condition, the computation of $\mathbf{L}$ under the wide-separation assumption for round conductors is given by [28, Eq. 5.23]

$$\mathbf{L} = \begin{bmatrix} \frac{\mu_0}{2\pi}\ln\left(\frac{d_{01}^2}{r_1 r_0}\right) & \frac{\mu_0}{2\pi}\ln\left(\frac{d_{01}d_{02}}{d_{12}r_0}\right) \\ \frac{\mu_0}{2\pi}\ln\left(\frac{d_{01}d_{02}}{d_{12}r_0}\right) & \frac{\mu_0}{2\pi}\ln\left(\frac{d_{02}^2}{r_2 r_0}\right) \end{bmatrix}, \tag{6}$$

where $\ln(\cdot)$ represents the natural logarithm and $d_{ij} = d_{\mathsf{cond}}$ (see Table I) is the separation between the ith and the jth conductor.

With the assumption of a homogeneous surrounding paper insulation, we use closed form approximations for the computation of $\mathbf{C}$ and $\mathbf{G}$ matrices to obtain [28, Eq. 5.24]

$$\mathbf{C} = \mu_0\epsilon_0\Re\{\epsilon_{\mathsf{PILC}}(\gamma)\}\mathbf{L}^{-1}, \tag{7}$$

$$\mathbf{G} = -2\pi f\mu_0\epsilon_0\Im\{\epsilon_{\mathsf{PILC}}(\gamma)\}\mathbf{L}^{-1}, \tag{8}$$

where $\epsilon_0 = 8.8 \times 10^{-12}$ H m^{-1} is the permittivity of free space. We then input the PUL parameters to an open-source PLC channel emulator [30] to generate CFRs for any given load condition and network architecture.

For an initial investigation, let us consider a simple network topology with no branches between the transmitter and the receiver. The transmitter is assumed to have a zero source impedance, which is consistent with a typically low transmit impedance used by PLC modems [31]. At the receiver-end of the line, we consider a general load condition as shown in Fig. 3. From Kirchhoff's current law, we obtain

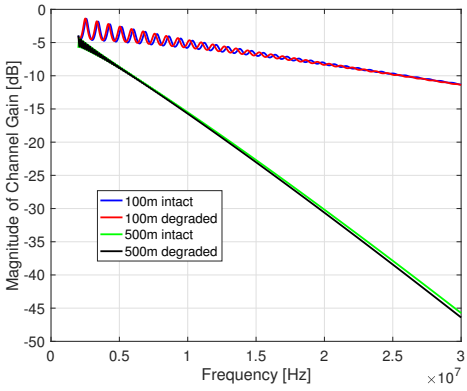

Fig. 4. CFR of intact and degraded cables of varying line lengths.

$$I_1 = \frac{V_1 - V_2}{Z_1} + \frac{V_1}{Z_0}, \tag{9}$$

$$I_2 = \frac{V_2 - V_1}{Z_1} + \frac{V_2}{Z_2}. \tag{10}$$

By simplifying (9) and (10), we represent

$$\begin{bmatrix} I_1 \\ I_2 \end{bmatrix} = \begin{bmatrix} \frac{1}{Z_0} + \frac{1}{Z_1} & -\frac{1}{Z_1} \\ -\frac{1}{Z_1} & \frac{1}{Z_2} + \frac{1}{Z_1} \end{bmatrix} \cdot \begin{bmatrix} V_1 \\ V_2 \end{bmatrix}. \tag{11}$$

Therefore, the load impedance matrix follows as

$$\mathbf{Z}_{\mathsf{L}} = \begin{bmatrix} \frac{1}{Z_0} + \frac{1}{Z_1} & -\frac{1}{Z_1} \\ -\frac{1}{Z_1} & \frac{1}{Z_2} + \frac{1}{Z_1} \end{bmatrix}^{-1}. \tag{12}$$

As an example, we consider the case where $Z_0 = Z_1 = Z_2 = 50\ \Omega$. The resulting CFRs for intact ($\gamma = 0$) and nominally degraded ($\gamma = 1$) cable conditions are presented in Fig. 4 for two line lengths of $\ell = 100$ m and $\ell = 500$ m. We observe that the thermal degradation causes a marginally higher signal attenuation due to the increased dielectric losses. However, apart from this insignificant difference, the nature of the response shows no noticeable differences irrespective of degradation for either of the two line lengths. Therefore, in Section IV, we present ML techniques that are able to capture these subtle deviations caused by the degradations, for different line lengths and varying load conditions. Furthermore, such solutions can be automated in real-world implementations to enable PLMs with intelligent grid diagnosis abilities.

IV. Machine Learning for Cable Diagnostics

In this section, we introduce the applied ML technique and the method of selecting the required features for training the machine, and present performance results of our proposed solution.

A. Cable Health Monitoring as a Regression Task

ML techniques have been used extensively for grid diagnostics, for e.g., in [8], [15], [20], [21]. Such techniques are highly beneficial, especially when sufficient data is available, but the

relationship between the input data (CFR, in our case) and the function to predict (γ, in our case), is complicated, specifically in our scenario, due to unknown and changing load conditions, and because of marginal differences between CFRs of healthy and degraded cables that are indistinguishable by manual inspection. Furthermore, once a machine is trained using cable CFRs with known degradation severity levels, it can then be loaded on to an operating PLM simply through software upgrades, and can also be regularly updated, if required.

We formulate the degradation severity assessment problem as a supervised learning task, where we use regression techniques in ML to predict the thermal degradation severity γ, using features extracted from the PLM-estimated CFRs. Among the various available regression methods, we use the least square boosting (LSBoost) technique, since LSBoost, as an ensemble learning algorithm that consolidates multiple weak learners into a strong learner, generally shows a good prediction performance and is less prone to over-fitting [32]. Specifically, when a total of N samples are used for training, LSBoost attempts to minimize the mean squared error

$$\Delta = \frac{1}{N}\sum_{i=1}^{N}(y(i) - f(\mathbf{x}_i))^2, \tag{13}$$

where $y(i)$ is the label associated with the data $\mathbf{x}_i$, and $f(\mathbf{x}_i)$ is the predicted label by the machine for $\mathbf{x}_i$. It uses the principle of gradient descent to iteratively minimize Δ beginning with an initial $f_{(0)}$. During each iteration, k ($k > 1$), the algorithm uses weak learners to approximate the gradient at $k-1$, $\Delta'_{(k-1)} = -\frac{2}{N}\sum_{i=1}^{N}(y(i) - f_{(k-1)}(\mathbf{x}_i))$, to get $\hat{\Delta}'_{(k-1)}$, and updates the prediction function $f_{(k)}$ with a chosen learning rate α, i.e., $f_{(k)} = f_{(k-1)} - \alpha\hat{\Delta}'_{(k-1)}$ [33, Ch. 16].

B. Feature Extraction

Selecting the right features is a crucial procedure that drives the performance of ML algorithms. From experience gained during our previous works [8], [15], we have learned that the moment statistics of the CFR, i.e., mean, variance, skewness, and kurtosis, computed across the operating bandwidth provide critical information to the machine to predict the state of the cable health. We can also observe in Fig. 4 that the CFR variance seems to be a distinguishing statistic since the degraded cable imposes slightly higher signal attenuation. Further, we know from the literature [15], [21] that the velocity of wave propagation is affected by cable degradations. Therefore, we also use the channel impulse response (CIR), and specifically, the peak locations in the CIR as features in our ML framework. These constitute our considered library for feature selection. For each ML task, different features present different degrees of importance, as will be presented in Section IV-C and Section V-B, where we select the most appropriate set of features that give the best performance.

C. Performance Evaluations

We test the effectiveness of our proposed schemes for two PILC cables, a long-run cable of 500 m, and a shorter 100 m cable. Since the dielectric property measurements are only available for $\gamma = 0$ and $\gamma = 1$ [24], in our evaluation, we extrapolate to obtain the relative permittivity of any degradation severity level as

$$\epsilon'_{\text{PILC}}(\gamma) = \epsilon'_{\text{PILC}}(1) + (1-\gamma)(\epsilon'_{\text{PILC}}(1) - \epsilon'_{\text{PILC}}(0)), \tag{14}$$

Note that γ does not necessarily vary linearly with the cable age under the accelerated or actual degradation. γ only indicates the degree of deterioration defined for our evaluations, with increasing values of γ representing an increase in the thermal degradation severity. Meanwhile, to emulate realistic load variations [34, Table 1.1], we generate random load conditions conforming to $Z_0,\ Z_1,\ Z_2 \sim (\mathscr{U}(0,50) + j\cdot\mathscr{U}(-50,50))\ \Omega$, where $\mathscr{U}(a,b)$ denotes a uniform distribution between a and b. To train and test the machine, we generated cable CFRs with varying degradation severities of $\gamma \sim \mathscr{U}(0,5)$.

To ensure satisfactory performance, we trained our machine with sufficient number of training samples of 3600. We then tested the accuracy of the trained machine with another 1000 different CFRs to obtain a noticeable performance trend. We show the resulting regression performance in Fig. 5 and Fig. 6. For both these tested scenarios, we notice that the fitted curve is essentially a straight line of unit slope passing through the origin. This substantiates that the prediction of our scheme is significantly accurate. Furthermore, all individual predictions are also in close proximity to the fitted line, displaying a

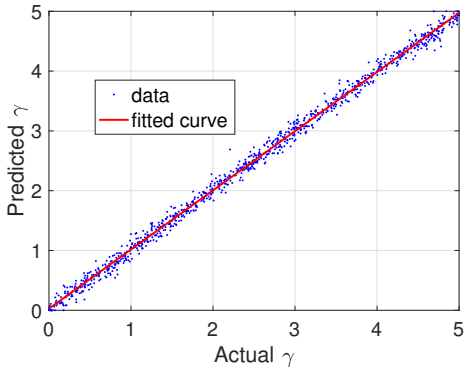

Fig. 5. Thermal degradation severity prediction results for a short cable of length 100 m.

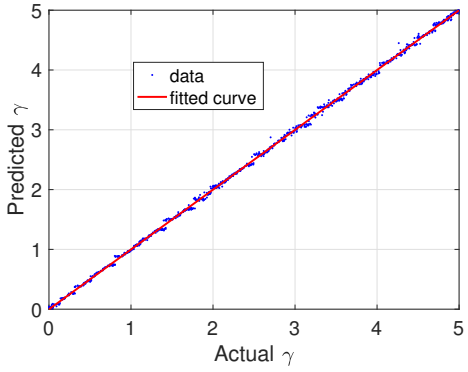

Fig. 6. Thermal degradation severity prediction results for a longer cable of length 500 m.

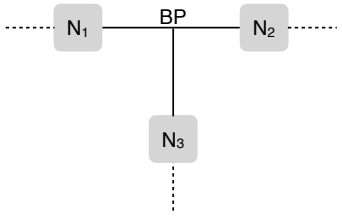

Fig. 7. A T-sub-network, which is part of a possibly more complicated distribution network.

relatively low prediction variance across different degradation severities.

In each of the two line length conditions, we choose the most appropriate set of features from the library specified in Section IV-B based on their usefulness in each test case. Specifically, for the results in Fig. 5, the first peak of the CIR, and variance and kurtosis of the CFR magnitude are mostly critical in descending order of importance. On the other hand, for the results in Fig. 6, the CFR magnitude variance and the skewness of the CIR are more crucial. Therefore, selecting useful features depend on the nature of the CFR and CIR under varying load conditions, type of cables, and line lengths. Thus, an oblivious selection of features from the literature, for e.g., choosing the same features as those used in, say [15], [21], does not guarantee yielding a satisfactory performance.

V. Discussion and Supplementary Results

In this section, we provide a brief discussion on our proposed solution and possible challenges that we could face in practical deployments.

A. General Network Topology and Cooperative Diagnostics

Throughout the evaluations in our paper, we have considered a rather simple network topology with no branches between the transmitter and the receiver. However, realistic LV networks typically have more complicated structures with multiple branches in between [35, Fig. 2.14], [13], [36]. For such networks, the topology can generally be decomposed into a concatenation of several T-networks. We have already shown the diagnostics procedure for elementary T-networks in our previous works [8], [15], following which, our proposed scheme can be extended to T-networks and thereby to other more general network architectures. At the same time, larger networks also have a larger number of PLMs available. In such cases, a cooperative diagnostics method can be applied for tackling the added network complexity. For example, consider the sub-network shown in Fig. 7, which is a part of a larger complicated LV distribution network. For a degradation assessment on, say, the $\mathsf{BP}-\mathsf{N}_3$ branch, CFRs from the other two nodes, N_1 and N_2, can also be used by N_3 to gain more insight into the situation of degradation. Such a scheme is also beneficial in avoiding topology ambiguities in the tasks, where the presence of a degradation or a line fault needs to be identified and localized. Naturally, cooperative diagnostics can be used to enhance prediction results for a simple topology as considered in Section IV as well.

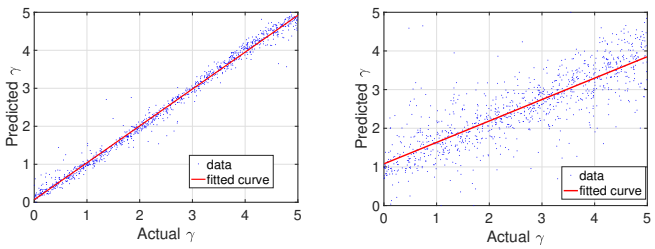

(a) 1500 m cable (b) 500 m cable

Fig. 8. Thermal degradation severity prediction results using NB-PLC CFRs.

B. Suitability for Narrowband PLC

Similar to the BB-PLC systems considered above, NB-PLC systems using frequency bands below 500 kHz [35, Ch.1, Ch. 9] can be used for cable health monitoring. First, we notice that the dielectric property changes in cable insulations due to thermal degradation are more pronounced at relatively lower frequencies [24]. Furthermore, NB-PLC systems are widely used for communication between smart meters and secondary transformers [22]. We thus also investigate the possibility of operating our proposed scheme under the NB-PLC scenario. Specifically, we conform with the PoweRline Intelligent Metering Evolution (PRIME) NB-PLC specifications and apply the CFRs for the PLC carriers between 41.9 kHz and 88.9 kHz lying within the CENELEC A-Band [37] as input to the same ML techniques discussed in Section IV.

With these NB-PLC settings, we trained and tested our machine with 3600 and 1000 samples, respectively, to obtain the results shown in Fig. 8, which shows the performance of our prediction for two different cables of lengths 1500 m and 500 m. For this scenario, we found the most useful features to be the kurtosis and skewness of the CTF phase.

While the fitted curve for the longer cable in Fig. 8 is still essentially a unit-slope line nearly passing through the origin, the prediction variance has noticeably increased when compared to the results obtained with BB-PLC (see Fig. 5 and Fig. 6). However, for the shorter cable, the performance with respect to prediction accuracy as well as variance of individual predictions are significantly degraded. These can be attributed to the new challenges introduced by using NB-PLC. First, since the operating frequency range and the available number of data sub-carriers are lower, we have a smaller data size per sample for training and testing our machine. Second, due to the large signal wavelength (over 1.8 km at 88.9 kHz) relative to the cable length, the noticeable sinusoidal fluctuations of CFR magnitude with frequency obfuscate the higher signal attenuations introduced by the degradation, which are clearly observable in the BB-PLC range due to the negligibility of such sinusoidal fluctuations. Therefore, the moment statistics computed using the CFR estimates are not as beneficial as in the case of BB-PLC. In conclusion, while our solution is applicable for cables of longer length under NB-PLC scenarios, prediction accuracy for shorter length cables could be challenging, as seen in Fig. 8.

C. Possible Limitations

For all our simulation evaluations, we have used the thermal degradation model based on the measurement results presented in [24] and its extrapolations at higher frequencies. Although this helps us in evaluating our scheme under different degradation severities, the comprehensiveness of the measurement campaign and the accuracy of the resulting model can only be verified through field trials to gauge the extent of possible emulation mismatches.

VI. Conclusion

In this paper, we have investigated thermal aging condition monitoring of paper insulated lead covered cables using power line modems. We have presented a machine learning based solution to endow power line modems with intelligent grid sensing abilities for automatic diagnostics by estimating thermal degradation severities in underground distribution cables of varying lengths under different network load conditions. Our proposed solution can be conducted online when the network is in full operation and can assist utilities in remotely monitoring the grid without requiring any additional dedicated equipments/components or dispatching technical personnel onsite. Our simulation evaluations have shown promising results with high accuracy and low prediction variance in degradation severity estimations. Finally, we have also presented techniques to extend our solution to larger LV/MV distribution networks with non-trivial network topologies and discussed feasibility of our proposed schemes using narrow-band power line communications.

References

[1] H. Orton, "History of underground power cables," *IEEE Electr. Insul. Mag.*, vol. 29, no. 4, pp. 52–57, 2013.

[2] P. Fairley, "Utilities bury more transmission lines to prevent storm damage," *IEEE Spectr.*, vol. 2, pp. 9–10, 2018.

[3] H. Farhangi, "The path of the smart grid," *IEEE Power Energy Mag.*, vol. 8, no. 1, pp. 18–28, 2010.

[4] "Economic benefits of increasing electric grid resilience to weather outages," *Washington, DC: Executive Office of the President*, 2013.

[5] T. Neier, "Cable diagnostic in MV underground cable networks: Theoretical background and practical application," https://www.pro-test.co.nz/site/pacifictestinstruments/files/PDF/Technical%20Pages/HV%20Cable%20testing%20and%20diagnostic%20Handbook%20.pdf, 2015.

[6] P. Werelius, *Development and application of high voltage dielectric spectroscopy for diagnosis of medium voltage XLPE cables*. PhD thesis, KTH, 2001.

[7] F. Yang, W. Ding, and J. Song, "Non-intrusive power line quality monitoring based on power line communications," in *Proc. IEEE Int. Symp. Power Line Commun. Appl. (ISPLC)*, pp. 191–196, 2013.

[8] L. Förstel and L. Lampe, "Grid diagnostics: Monitoring cable aging using power line transmission," in *Proc. IEEE Int. Symp. Power Line Commun. Appl. (ISPLC)*, pp. 1–6, 2017.

[9] Itron, "Openway powered by itron riva technology," https://www1.itron.com/Documents/OpenWay-Riva.pdf, 2014.

[10] S. Galli, A. Scaglione, and Z. Wang, "For the grid and through the grid: The role of power line communications in the smart grid," *Proc. IEEE*, vol. 99, no. 6, pp. 998–1027, 2011.

[11] V. C. Gungor, D. Sahin, T. Kocak, S. Ergut, C. Buccella, C. Cecati, and G. P. Hancke, "Smart grid technologies: Communication technologies and standards," *IEEE Trans. Ind. Informat.*, vol. 7, no. 4, pp. 529–539, 2011.

[12] M. Ahmed and W. L. Soo, "Power line carrier (PLC) based communication system for distribution automation system," in *IEEE Int. Power and Energy Conf.*, pp. 1638–1643, 2008.

[13] A. Mengi, S. Ponzelar, and M. Koch, "The ITU-T G.9960 broadband PLC communication concept for smartgrid applications," in *IEEE Int. Conf. on Smart Grid Commun. (SmartGridComm)*, pp. 492–496, Oct 2017.

[14] J. Densley, "Ageing mechanisms and diagnostics for power cables - an overview," *IEEE Electr. Insul. Mag.*, vol. 17, no. 1, pp. 14–22, 2001.

[15] Y. Huo, G. Prasad, L. Atanackovic, L. Lampe, and V. C. M. Leung, "Grid surveillance and diagnostics using power line communications," in *Proc. IEEE Int. Symp. Power Line Commun. Appl. (ISPLC)*, pp. 1–6, 2018.

[16] W. Shu, J. Guo, and S. A. Boggs, "Water treeing in low voltage cables," *IEEE Electr. Insul. Mag.*, vol. 29, no. 2, pp. 63–68, 2013.

[17] W. Lawson, M. Simmons, and P. Gale, "Thermal ageing of cellulose paper insulation," *IEEE Trans. Electr. Insul.*, no. 1, pp. 61–66, 1977.

[18] I. Mladenovic and C. Weindl, "Artificial aging and diagnostic measurements on medium-voltage, paper-insulated, lead-covered cables," *IEEE Electr. Insul. Mag.*, vol. 28, no. 1, 2012.

[19] F. Eppelein, C. Weindl, and I. Mladenovic, "Analysis and evaluation of dielectric parameters for design verification and calibration of a newly developed diagnostic system for mv power cables," *CIRED-Open Access Proc. J.*, vol. 2017, no. 1, pp. 10–14, 2017.

[20] T. S. Abdelgayed, W. G. Morsi, and T. S. Sidhu, "Fault detection and classification based on co-training of semisupervised machine learning," *IEEE Trans. Ind. Electron.*, vol. 65, no. 2, pp. 1595–1605, 2018.

[21] H. Livani and C. Y. Evrenosoglu, "A machine learning and wavelet-based fault location method for hybrid transmission lines," *IEEE Trans. Smart Grid*, vol. 5, no. 1, pp. 51–59, 2014.

[22] A. Sendin, T. Arzuaga, I. Urrutia, I. Berganza, A. Fernandez, L. Marron, A. Llano, and A. Arzuaga, "Adaptation of powerline communications-based smart metering deployments to the requirements of smart grids," *Energies*, vol. 8, no. 12, pp. 13481–13507, 2015.

[23] E. Brancato, "Insulation aging a historical and critical review," *IEEE Trans. Electr. Insul.*, no. 4, pp. 308–317, 1978.

[24] R. Liao, J. Hao, G. Chen, and L. Yang, "Quantitative analysis of ageing condition of oil-paper insulation by frequency domain spectroscopy," *IEEE Trans. Dielectr. Electr. Insul.*, vol. 19, no. 3, 2012.

[25] "IEEE standard for broadband over power line networks: Medium access control and physical layer specifications," *IEEE Std 1901-2010*, pp. 1–1586, 2010.

[26] "Homeplug green PHY specification," *HomePlug Powerline Alliance*, 2010.

[27] F. Versolatto and A. M. Tonello, "An MTL theory approach for the simulation of MIMO power-line communication channels," *IEEE Trans. Power Del.*, vol. 26, no. 3, pp. 1710–1717, 2011.

[28] C. R. Paul, *Analysis of multiconductor transmission lines*. John Wiley & Sons, 2008.

[29] BATTCABLES, "Three-conductor PILC mains power distribution cable BS6480," http://www.batt.co.uk/upload/files/pilc3corepaperleadswapvc635011000vbs6480_1317052209.pdf.

[30] F. Gruber and L. Lampe, "On PLC channel emulation via transmission line theory," in *Proc. IEEE Int. Symp. Power Line Commun. Appl. (ISPLC)*, pp. 178–183, 2015.

[31] "Integrated powerline communication analog front-end transceiver and line driver," http://www.maximic.com/datasheet/index.mvp/id/6333.

[32] Y. Freund and R. Schapire, "A short introduction to boosting," *Jpn. Soc. Artificial Intell.*, vol. 14, no. 5, pp. 771–780, 1999.

[33] K. Murphy, *Machine Learning: A Probabilistic Perspective*. Adaptive computation and machine learning, MIT Press, 2012.

[34] L. T. Berger, A. Schwager, P. Pagani, and D. Schneider, *MIMO power line communications: narrow and broadband standards, EMC, and advanced processing*. CRC Press, 2014.

[35] L. Lampe, A. M. Tonello, and T. G. Swart, *Power Line Communications: Principles, Standards and Applications from Multimedia to Smart Grid*. John Wiley & Sons, 2016.

[36] G. S. Prasanna, A. Lakshmi, S. Sumanth, V. Simha, J. Bapat, and G. Koomullil, "Data communication over the smart grid," in *Proc. IEEE Int. Symp. Power Line Commun. Appl. (ISPLC)*, pp. 273–279, 2009.

[37] "PRIME v1.4 specifications," standard, PRIME Alliance, Nov., 2014.